Characterizing the conformational dynamics of metal-free PsaA using molecular dynamics simulations and electron paramagnetic resonance spectroscopy

Supplementary Material

Evelyne Deplazes [1,2,‡], Stephanie L. Begg [3,‡], Jessica H. van Wonderen [4‡], Rebecca Campbell [3], Bostjan Kobe [1,2,5], James C. Paton [3], Fraser MacMillan [4], Christopher A. McDevitt [3,], Megan L. O'Mara [1,6,*]*

[1] School of Chemistry and Molecular Biosciences, The University of Queensland, Brisbane, Australia.

[2] Institute for Molecular Bioscience, The University of Queensland, Brisbane, Australia.

[3] Research Centre for Infectious Diseases, School of Biological Sciences, University of Adelaide, Adelaide, Australia.

[4] Henry Wellcome Unit for Biological EPR, School of Chemistry, Norwich Research Park, University of East Anglia, Norwich, UK

[5] Australian Infectious Diseases Research Centre, University of Queensland, Brisbane, Australia

[6] Research School of Chemistry, The Australian National University, Canberra, Australia.

‡ ED, SB and JHW contributed equally to this work.

*Corresponding Authors:

E-mail: megan.o'mara@anu.edu.au E-mail: christopher.mcdevitt@adelaide.edu.au

Supplementary Table S1. Primary sequence of PsaA (from PDBid 3Z7K, chain A) used in the EPR and MD simulations of this study.

KLKVVATNSIIADITKNIAGDKIDLHSIVPIGQDPHEYEPLPEDVKKTSEADLIFYNGINLETGGNAWFTKLVENAKKTE
NKDYFAVSDGVDVIYLEGQNEKGKEDPHAWLNLENGIIFAKNIAKQLSAKDPNNKEFYEKNLKEYTDKLDKLDKESKDKF
NKIPAEKKLIVTSEGAFKYFSKAYGVPSAYIWEINTEEEGTPEQIKTLVEKLRQTKVPSLFVESSVDDRPMKTVSQDTNI
PIYAQIFTNSIAEQGKEGDSYYSMMKYNLDKIAEGLAK

Supplementary Table S2. Oligonucleotide primers used in this study

Primer	Sequence (5'-3')
L56C-PsaA_F	aaatattgctggtgacaaaattgactgccatagtatcgttccgattgggcaag
L56C-PsaA_R	cttgcccaatcggaacgatactatggcagtcaattttgtcaccagcaatattt
S58C-PsaA_F	ttgctggtgacaaaattgaccttcattgcatcgttccgattgg
S56C-PsaA_R	ccaatcggaacgatgcaatgaaggtcaattttgtcaccagcaa
I125C-PsaA_F	cagcgacggcgttgatgtttgctaccttgaaggtcaaaat
I125C-PsaA_R	attttgaccttcaaggtagcaaacatcaacgccgtcgctg
I236C-PsaA_F	aagaagaaggaactcctgaacaatgcaagaccttggttgaaaaacttc
I236C-PsaA_R	gaagtttttcaaccaaggtcttgcattgttcaggagttccttcttctt
S266C-PsaA_F	tggatgaccgtccaatgaaaactgtttgccaagacacaaacatc
S266C-PsaA_R	gatgtttgtgtcttggcaaacagttttcattggacggtcatcca

Supplementary Table S3. Comparison of inter-residue distances in the metal coordination site of Mn-bound PsaA and metal-free PsaA in solution. Inter-residue distances for the Mn-bound PsaA are taken from the respective crystal structures. Distances for the different conformations of metal-free PsaA in solution are extracted using a series of structures from the MD simulations representative of the conformations in the four most populated clusters.

PsaA conformation	δ His67-N – Glu205-O (Å)	δ His139-N – Asp280-O (Å)
Mn-bound, closed (3ZTT) [1]	3.1	2.9
Mn-bound, open* (3ZKA, PsaAD280N) [2]	4.6	7.6
Metal-free PsaA (3KZ7) [2]	5.9	8.2
Metal-free PsaA, cluster 1 (dominant conformation)	12.7 ± 2.2	6.4 ± 1.2
Metal-free PsaA, cluster 2	17.6 ± 2.4	5.6 ± 1.3
Metal-free PsaA, cluster 3	12.1 ± 1.6	5.3 ± 1.4
Metal-free PsaA, cluster 4	13.3 ± 2.7	12.2 ± 1.8

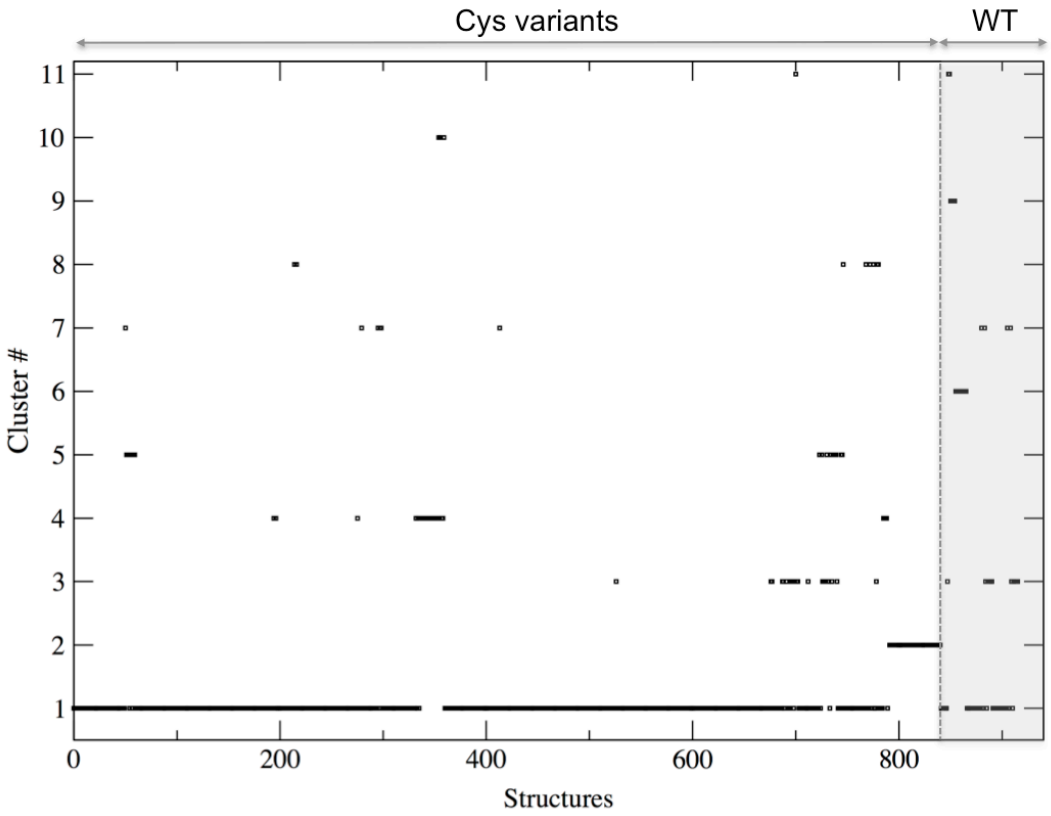

Supplementary Figure S1: Clustering of PsaA structures in solution. 840 structures from simulations of the five Cys-PsaA variants and 80 structures from simulations of wild-type PsaA were combined and clustered using a 0.25 nm cut-off resulting in 11 clusters (with 2 ore more structures). The number of structures in each cluster are: cluster 1, 82%; cluster 2, 5%; cluster 3, 4%; cluster 4, 3%; cluster 5, 2%, cluster 6,7 and 8, 1% each and cluster 9, 10 and 11 <1% each. Structures from WT simulations are found in clusters 1,3, 6, 7, 9 and 11. Structures from both WT and all five Cys-PsaA variants are found in the dominant cluster (cluster 1) while structures from WT simulations are found in clusters 1,3, 4, 6, 7, 9 and 11.

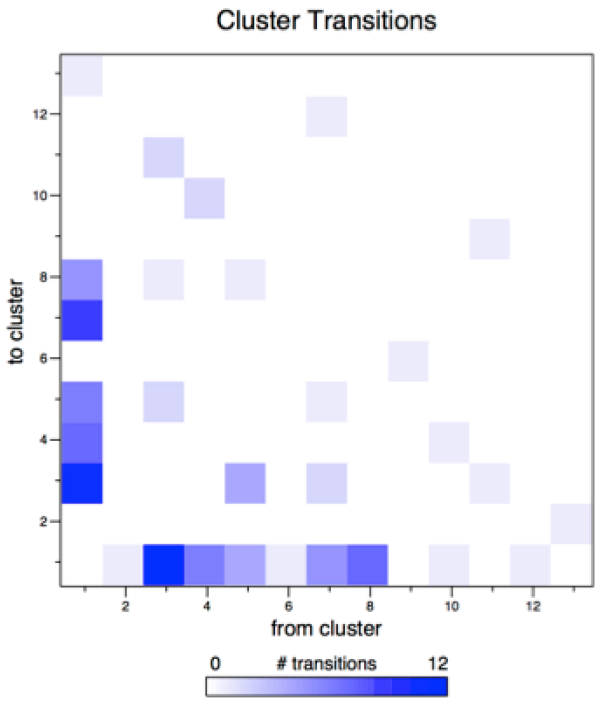

Cluster	# Transitions
1	77
2	2
3	35
4	16
5	18
6	2
7	18
8	14
9	2
10	4
11	4
12	2
13	2

Supplementary Figure S2: Transitions between clusters of PsaA in solution from cluster analysis of simulations of wild-type PsaA. 840 structures from simulations of the five Cys-PsaA variants and 80 structures from simulations of wild-type PsaA were combined and clustered using a 0.25 nm cut-off resulting in 11 clusters with 2 ore more structures (cluster 12 and 13 contain only 1 structure each). There are a large number of transitions to and from clusters 1, 3, 4, 5, 7 and 8, which together contain more than 93% of structures.

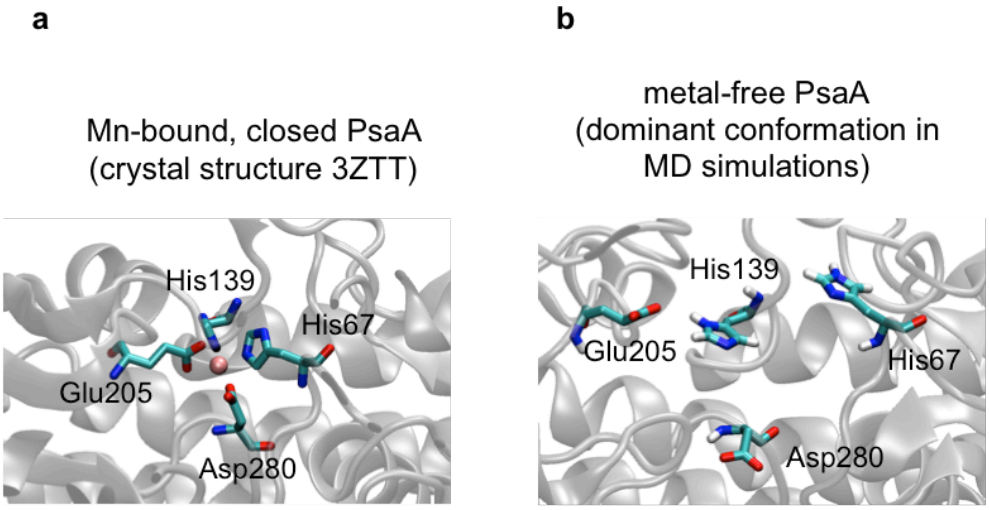

Supplementary Figure S3: Comparison of metal coordination site in Mn-bound and metal-free PsaA. (a) In the Mn-bound PsaA, the metal is coordinated by the side chains of residues His139, His67, Asp280 and Glu205. (b) In the dominant conformation from the MD simulations of metal-free PsaA in solution, the inter-residue distance between His67 and Glu205 is significantly higher. In none of the conformations sampled in the MD simulations of metal-free PsaA in solution are the residues close enough to coordinate a metal ion. See also the inter-residue distances provided in Table S2.

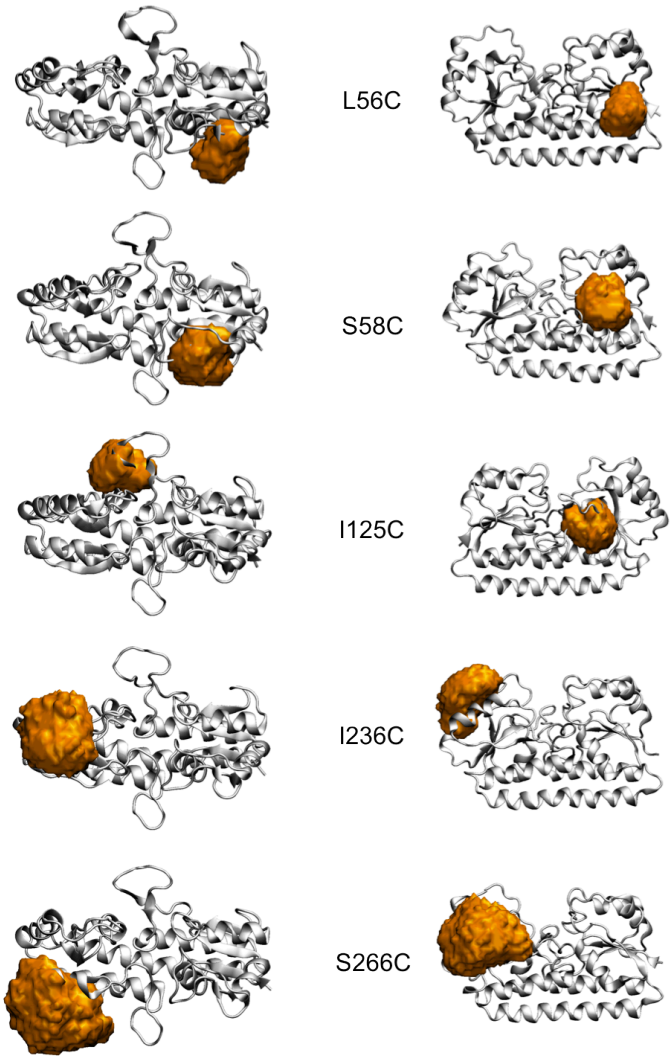

Supplementary Figure S4: Volumetric maps of the MTSL spin labels in the five different Cys-PsaA variants. The volumetric maps (orange) show the occupancy of the MTSL probe throughout the 3 × 300ns of unrestrained MD simulation of each of the five Cys-PsaA variants.

References

1 McDevitt, C. A. *et al.* A molecular mechanism for bacterial susceptibility to zinc. *PLoS Pathog.* **7**, e1002357, (2011).

2 Counago, R. M. *et al.* Imperfect coordination chemistry facilitates metal ion release in the psa permease. *Nat. Chem. Biol.* **10**, 35-41, (2014).